Title

Adenovirus E1A binding to DCAF10 targets proteasomal degradation of RUVBL1/2 AAA+ ATPases required for quaternary assembly of multiprotein machines, innate immunity, and responses to metabolic stress

Journal

Journal of Virology, 97(12)

ISSN

0022-538X

Authors

Zemke, Nathan R
Hsu, Emily
Barshop, William D
et al.

Publication Date

2023-12-21

DOI

10.1128/jvi.00993-23

Peer reviewed

AMERICAN SOCIETY FOR MICROBIOLOGY | Journal of Virology

Editor's Pick | Virology | Full-Length Text

Adenovirus E1A binding to DCAF10 targets proteasomal degradation of RUVBL1/2 AAA+ ATPases required for quaternary assembly of multiprotein machines, innate immunity, and responses to metabolic stress

Nathan R. Zemke,[1,2,3] Emily Hsu,[1,3,4] William D. Barshop,[5,6] Jihui Sha,[5] James A. Wohlschlegel,[1,5] Arnold J. Berk[1,3]

AUTHOR AFFILIATIONS See affiliation list on p. 17.

ABSTRACT Adenovirus small e1a protein modifies host cell physiology to optimize virus replication. The N-terminal ~140 aa of e1a interacts with RB-family proteins to derepress dNTP and DNA synthesis and with EP300/CREBBP lysine acetyltransferases and EP400-TIP60 chromatin-modifying complexes to inhibit host anti-viral innate immune responses. However, the e1a N-terminal region activates a late host anti-viral response due to stabilization and activation of IRF3. The E1A C-terminal region counteracts IRF3 stabilization through interactions with three host nuclear proteins with seemingly unrelated functions. All three C-terminal interactions are required for e1a-association into a multi-protein complex with scaffold subunits of a CRL4 E3 ubiquitin ligase and DCAF10, a presumed specificity subunit. This e1a-DCAF10-CRL4 prevents IRF3 stabilization indirectly by targeting the essential AAA+ ATPases RUVBL1/2, subunits of several HSP90 co-chaperones required for quaternary assembly of cellular protein machines required for anti-viral defenses and responses to genotoxic and metabolic stress.

IMPORTANCE Inactivation of EP300/CREBB paralogous cellular lysine acetyltransferases (KATs) during the early phase of infection is a consistent feature of DNA viruses. The cell responds by stabilizing transcription factor IRF3 which activates transcription of scores of interferon-stimulated genes (ISGs), inhibiting viral replication. Human respiratory adenoviruses counter this by assembling a CUL4-based ubiquitin ligase complex that polyubiquitinylates RUVBL1 and 2 inducing their proteasomal degradation. This inhibits accumulation of active IRF3 and the expression of anti-viral ISGs, allowing replication of the respiratory HAdVs in the face of inhibition of EP300/CBEBBP KAT activity by the N-terminal region of E1A.

KEYWORDS adenovirus, E1A, IRF3, DCAF10, CRL4, innate immunity, virology, P300, CBP

Human adenoviruses HAdV-C2 and HAdV-C5 are closely related DNA tumor viruses that infect the ciliated pseudostratified columnar epithelial cells covering the air-tissue interface of the upper respiratory tract. To produce maximum progeny, these respiratory adenoviruses repress host innate anti-viral immune responses (1, 2) and force terminally differentiated, G_0-arrested host cells into S-phase to achieve high rates of viral DNA replication (3–6). Two major E1A protein isoforms are the first viral proteins expressed after infection (3): large E1A, 289 amino acids and small e1a, 243 amino acids (7). Large E1A contains an ~60 amino acid transcriptional activation domain near the middle of the protein that activates transcription of viral early genes (3, 6, 8). Small e1a lacks the transcriptional activation domain but is sufficient to force G_0-arrested cells into S-phase (3–5). This activity of E1A/e1a promotes oncogenic transformation

Editor Lawrence Banks, International Centre for Genetic Engineering and Biotechnology, Trieste, Italy

Address correspondence to Arnold J. Berk, arnold.berk@icloud.com.

The authors declare no conflict of interest.

Received 8 July 2023
Accepted 16 October 2023
Published 14 November 2023

of cultured primary mammalian cells when cooperating with other oncogenes such as G12V *H-RAS* (9) or either of the HAdV-C5 major E1B proteins (10, 11). Conserved regions in e1a's N-terminal half activate cell cycle genes by binding and inhibiting RB-family proteins (RBs) (12–16). Additional conserved peptides in the N-terminal half of e1a repress innate anti-viral defense genes by binding and inhibiting the closely related nuclear lysine-acetyl transferases (KATs) EP300 and CREBBP (14, 16) and the ~20 subunit TIP60 chromatin-modifying complexes containing the EP400 helicase (17) and TIP60 KATs (18, 19). While much is understood about the conserved N-terminal regions of E1A/e1a referred to as CR1 and CR2 (Fig. S1), much less is known about the functions of three conserved peptides in the C-terminal region (~120 amino acids) (20) diagrammed in orange, pink, and blue in Fig. S1 and how they contribute to virus fitness.

Members of three distinct cellular protein families bind the three conserved peptides in the C-terminal region of E1A proteins (21). All are encoded in the second exon of the two major E1A mRNAs (7) expressed during the early phase of infection before the onset of viral DNA replication. These peptides are bound by the paralogous transcription factors FOXK1 and FOXK2 at a conserved serine/threonine-rich region of E1A/e1a between amino acids 169 and 193 (large E1A numbering) (orange in Fig. S1) via their FHA (forkhead-associated) domain that binds phospho-Ser/Thr-containing peptides (22, 23). E1A peptide 202–227 (pink in Fig. S1) is bound by cellular protein DCAF7 and associated protein kinases DYRK1A, DYRK1B, and HIPK2 (23, 24). The paralogous transcriptional co-repressors CtBP1 and CtBP2 bind to the conserved PXDLS CtBP-binding motif near e1a's C-terminus (blue in Fig. S1) (25, 26). These three interactions are mediated through distinct e1a regions allowing for mutational disruption of any single interaction without interfering with the other two (21).

We reported previously on gene expression changes in primary human bronchial/tracheal epithelial cells (HBTECs) after HAdV infection (21). These G0-arrested, confluent primary HBTECs are a cell culture model of the human respiratory epithelium, which the human group C adenoviruses infect in nature. HBTECs were infected with HAdV-C5 vectors expressing wild-type e1a or e1a mutants defective for binding FOXK transcription factors, DCAF7 protein kinase complexes, or CtBP1 and 2. In addition to the dramatic changes in host cell gene expression regulated by the N-terminal half of E1A that stimulate cell growth and replication, these e1a C-terminal mutants activated expression of ~50 interferon-stimulated genes (ISGs) (21). Despite interacting with three host nuclear proteins with no known related functions (Fig. S1), each of these e1a C-terminal mutants caused stabilization and activating phosphorylation of IRF3 (21), a sequence-specific DNA-binding activator of ISGs (27, 28). After the expression of e1a C-terminal mutants, IRF3 was imported from its repressed cytoplasmic localization in unstimulated cells into nuclei during a "late interferon response" (29). In the nucleus, activated IRF3 binds interferon response elements in the promoter regions of target genes and activates high rates of ISG transcription (21).

Importantly, infection with the E1A deletion mutant *dl*312 (30) did not induce most of these ISGs even though its viral DNA is transported into nuclei of infected cells using the normal HAdV-C5 infectious process (31). The observation that many ISGs were induced by the e1a C-terminal mutants, but not by infection with *dl*312, indicated that this late innate immune response (29) is triggered by the expression of the C-terminal e1a mutant proteins and not by the detection of adenovirus nucleic acids exposed during infection. These observations led us to investigate how the e1a C-terminal mutant proteins induce IRF3 stabilization and how IRF3 stabilization is prevented by e1a C-terminal region interactions with FOXK1/2, DCAF7, and CtBP1/2.

Here, we report that e1a inhibition of EP300 and CREBBP KAT activities by the N-terminal half of the e1a C-terminal mutants induces IRF3 stabilization and activation. WT e1a counters this IRF3 stabilization by assembling a ubiquitin ligase with presumed host cell specificity factor DCAF10. This large complex assembled by WT e1a induces proteasomal degradation of IRF3, e1a itself, and the essential host cell helicases RUVBL1 and RUVBL2. RUVBL1 and RUVBL2 are required for maximal activation of ISGs in response

to interferon (32, 33). They are also essential subunits of the TIP60-containing chromatin-modifying complexes as well as several HSP90 co-chaperones required for the quaternary assembly of cellular "multi-protein machines" involved in host cell anti-viral defenses and responses to genotoxic and metabolic stresses (34). Our results reveal new insights into how RUVBL1/2 HSP90 co-chaperones promote anti-viral defense responses and how the three conserved C-terminal regions of the E1A proteins cooperate to inhibit the anti-viral response induced by the oncogenic N-terminal half of E1A during the "epic battle" between virus and host.

RESULTS

Adenovirus e1a C-terminal mutants activate an innate immune response

To assess the influence of interactions of conserved peptides in the C-terminal region of e1a with host proteins, we constructed HAdV-C5 vectors (35) that express WT e1a or an e1a C-terminal region mutant with two or four amino acid substitutions that completely block detectable e1a binding to FOXK1/2 (T229A, S231A, large E1A numbering), DCAF7 complexes (R258E, D271K, L272A, L273A), or CtBP1/2 (PLDLS to ALAAA at amino acids 279–283) (Fig. S1) (21). We used amino acid substitutions to block host cell protein binding rather than deletions so that the precise spacing between the remaining host protein binding sites was not altered (21). These C-terminal mutant vectors were named, respectively, "FOXKb$^-$," "DCAF7b$^-$," and "CtBPb$^-$." To inhibit the expression of all other HAdV-C5 genes before 24 h post infection (hpi), these vectors did not express large E1A, the principal E1A transcriptional activator of the early viral genes (3, 6), because of a 9 bp deletion that removes the 5′ splice-site required for producing the 13S E1A mRNA encoding the large E1A protein isoform. As a result, these vectors express small e1a but are defective for the expression of all other viral proteins before 24 hpi (3).

RNA-seq of G_0-arrested primary human respiratory tract epithelial cells (HBTECs) at 24 hpi with these vectors identified 52 host cell genes activated >5-fold by all three of these distinct e1a C-terminal mutants (FOXKb$^-$, DCAF7b$^-$, and CtBPb$^-$) (21) (Fig. 1A) (GEO accession GSE105039). These genes are >90% reported ISGs with established anti-viral activities (21). Most of these genes (33/52) were not activated by infection with the E1A deletion mutant *dl*312 (30) (Fig. 1A, top cluster: e1a C-terminal mutant responsive). The activation of ISGs coincided with an increase in IRF3 protein (Fig. 1B) without a corresponding increase in IRF3 mRNA (Fig. 1C), consistent with IRF3 protein stabilization shown previously with 35S-Met/Cys pulse-chase radio-labeling experiments (21). An siRNA knockdown (KD) of IRF3 greatly reduced the ability of DCAF7b$^-$ e1a to activate IRF3 target genes *IFIT2*, *OASL*, or *MX1* (Fig. 1D). Thus, the e1a C-terminal mutants trigger a "late interferon response" (29) in infected HBTECs by stabilizing IRF3 by a mechanism that is not triggered by viral DNA alone (since it is not triggered by infection with *dl*312) but rather by the expression of the C-terminal e1a mutant proteins. Furthermore, earlier co-infection assays indicated that a single e1a molecule must interact with FOXK1/2, DCAF7, and CtBP1/2 to inhibit the late interferon response since e1a C-terminal mutant co-infections did not complement to phenocopy wild-type e1a (21).

Inhibition of EP300/CREBBP acetyl transferase activities triggers IRF3 stabilization

Most of e1a's ability to regulate transcription of the viral and host cell genomes is credited to interactions of peptides conserved between the ~50 different primate adenoviruses (20) in the intrinsically disordered N-terminal half of e1a (13, 14). This region of e1a interacts with RB family proteins (12–15), EP300/CREBBP (14), and EP400/TIP60-containing chromatin remodeling complexes (Fig. S1) (17–19).To determine if any of the interactions of the N-terminal half of e1a are necessary for IRF3 stabilization in response to the e1a C-terminal mutations, we constructed three HAdV-C5 vectors that express double-interaction mutants of e1a: e1a defective in binding both DCAF7 and the closely related KAT paralogs EP300 and CREBBP (P300b$^-$/DCAF7b$^-$), e1a defective in

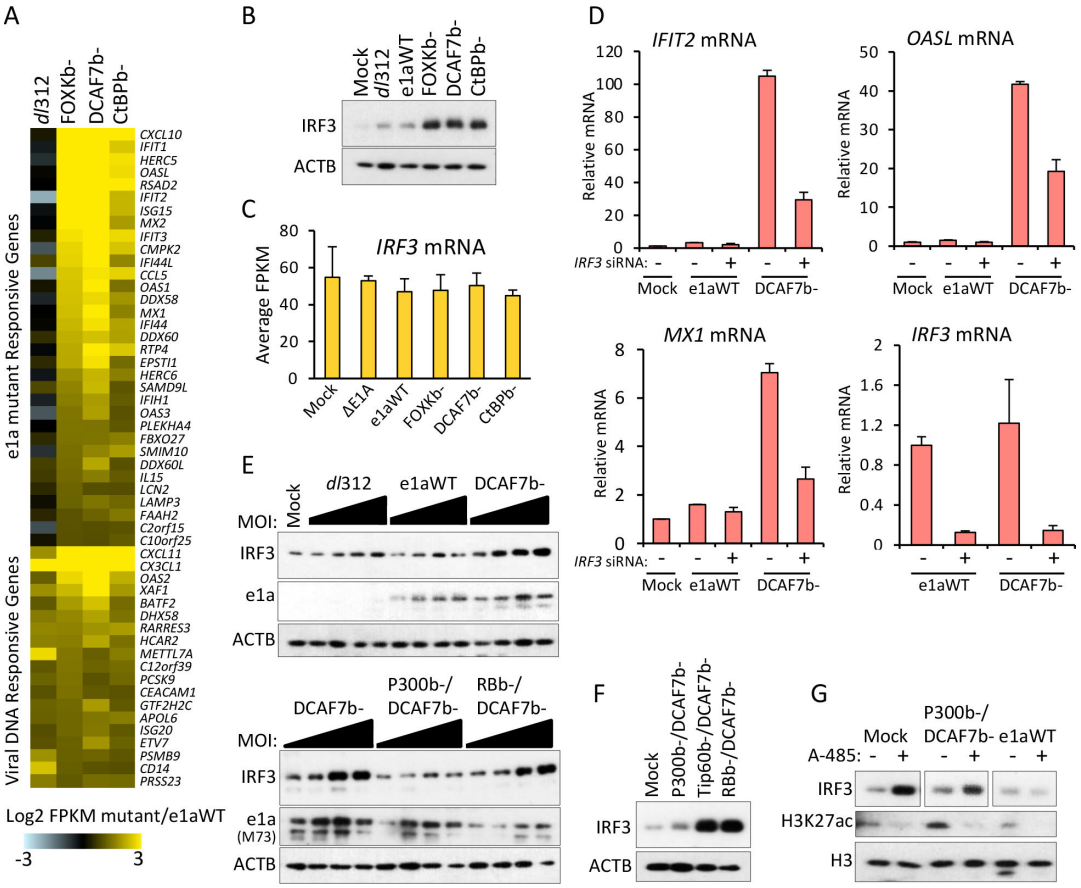

FIG 1 e1a inhibition of E300/CBP lysine-acetyl transferase activity induces IRF3 stabilization. (A) Heatmap displaying changes in RNA-seq FPKM of 52 host genes In G_0-arrested primary HBTECs that are activated by infection with the e1a C-terminal mutant expression vectors compared to cells infected with the e1aWT vector. Cluster 1 = e1 a C-terminal mutant responsive genes activated >5-fold by the expression of the e1a C-terminal mutants, but <2-fold by infection with the E1A deletion mutant *dl*312 (35). Cluster 2 = genes activated >2-fold by the expression of the e1a C-terminal mutants and by infection with *dl*312. (B) Western blots of HBTECs 24 hpi with the Ad5 vectors indicated at the top. (C) qRT-PCR with RNA extracted from HBTECs 24 hpi with Ad5 vectors indicated at the top. (D) qRT-PCR with RNA from HBTECs transfected for 2 days with the indicated siRNAs and then infected with Ad5 vectors indicated at the top for an additional 24 h. (E) Western blots of HBTECs infected with the indicated vectors at increasing MOI: 20, 60, 100, 140. (F) Western blots of protein isolated 24 hpi with HAdV-C5 vectors expressing the e1a mutants indicated at the top. (G) Western blots of protein from HBTECs infected for 12 h with vectors expressing the indicated double e1a mutants, followed by the addition of DMSO or 10 µM A485 for an additional 12 h (averages of three experimental replicates + SD). In D and G, "–" indicates results from cells transfected with the negative control siRNA (siCtrl).

binding both DCAF7 and the three RB paralogs (RBb$^-$/DCAF7b$^-$), and e1a defective in binding both DCAF7 and TIP60 complexes (TIP60b$^-$/DCAF7b$^-$). Infection of HBTECs with increasing moi (20–140) of *dl*312 (ΔE1A) or the vector expressing wild-type small e1a (e1aWT) had only modest effects on IRF3 level (Fig. 1E upper). But, as before (Fig. 1B), infection with increasing moi of the Ad vector for the DCAF7b$^-$ e1a mutant increased the level of IRF3 protein more (Fig. 1E, upper). RBb$^-$/DCAF7b$^-$ and TIP60b$^-$/DCAF7b$^-$ e1a also induced IRF3 accumulation (Fig. 1F). However, the P300b$^-$/DCAF7b$^-$ e1a mutant induced much less accumulation of IRF3 protein (Fig. 1E lower, 1F). We conclude that the e1a C-terminal mutants must bind CREBBP and EP300 through their N-terminus and CR1 (Fig. S1) to induce IRF3 stabilization, but binding to either RBs or TIP60 complexes is not necessary to induce IRF3 stabilization.

Small e1a binds directly to EP300 and CREBBP and inhibits their KAT activities (14, 16). To determine if inhibition of EP300 and CREBBP KAT activities is responsible for increasing IRF3 stability in cells infected with the e1a C-terminal mutants, we performed experiments with A485, a potent small-molecule competitive inhibitor of acetyl CoA binding to EP300 and CREBBP with exquisite specificity for binding to EP300 and CREBBP

as opposed to acetyltransferases in other structural classes such as PCAF (KAT2B) and GCN5 (KAT2A) (36). As expected, EP300 and CREBBP-mediated acetylation of histone H3 lysine 27 (H3K27ac) was greatly reduced by A485 treatment for 12 h (Fig. 1G, two lower rows). These results indicate that inhibition of EP300 and CREBBP KAT activities either by the N-terminal half of e1a or by treatment with A485 induces IRF3 stabilization. Since WT e1a inhibits EP300 and CREBBP KAT activity but does not increase IRF3 stability (Fig. 1G), we hypothesized that WT e1a has an additional activity that prevents IRF3 stabilization in response to the inhibition of EP300 and CREBBP KAT activity, but this activity is lost when any one of the C-terminal e1a interactions with host proteins fails to occur.

Interactomes of WT e1a and e1a C-terminal mutants

To investigate why e1a C-terminal mutants stabilize IRF3, but WT e1a does not, we compared proteins bound by WT e1a and the C-terminal mutants by co-immunoprecipitation (co-IP) followed by mass spectrometry. A549 cells derived from a human bronchial carcinoma (37) were infected with the HAdV-C5 vectors expressing WT e1a or a C-terminal e1a mutant. Cell lysates were immunoprecipitated with a monoclonal antibody (M58) that binds an epitope in e1a's N terminal half (38). Mass spec results confirmed specific disruption of FOXK TF-binding to the FOXKb– e1a mutant, DCAF7 and DYRK1A/B binding to the DCAF7b– e1a mutant, and CtBP1 or CtBP2 binding to the CtBPb– e1a mutants. (Fig. 2A). Host proteins that bind to peptides in the N-terminal half of e1a (CBP, EP300, RB, RBL1, RBL2, TRRAP, and EP400) were all enriched in M58 anti-e1a IPs of extracts from cells infected with the WT e1a and C-terminal mutant vectors compared to mock-infected cells (Fig. 2A; Table S1). This confirmed that WT e1a, C-terminal e1a mutants, and their associated proteins were all specifically immunoprecipitated by M58. Because of these positive internal controls with host proteins that bind to the N-terminal half of e1a, the absence of a host protein co-IPed with WTe1a from an IP of cells infected with a C-terminal mutant vector indicates that the mutant does not bind the identified protein. Other previously reported e1a interacting proteins were also detected in the M58 IPs such as MYC (39) and 26S proteasome subunits (40).

The 191 host proteins that co-IPed with the C-terminal mutants were significantly enriched for known protein-protein interactions compared to random proteins ($P < 1e{-}6$, Fig. 2B). Enriched KEGG pathways gene ontology terms associated with the specifically IPed proteins include cell cycle, pathways in cancer, TGFβ signaling, mismatch repair, carcinogenesis, proteasome, and spliceosome (Fig. 2B). Among the proteins not previously reported to associate with E1A/e1a were PRKDC, KS6A4, DCAF10, U119A, and ZYG11B (UniProtKB names, Table S1). PRKDC is the catalytic subunit of DNA-PK, a protein kinase in a large complex involved in double-stranded DNA break repair whose function is antagonized by e1a (41). KS6A4S, also known as Ribosomal protein S6 kinase alpha-4 , and PRDKC co-IPed with WT e1a, the FOXKb– e1a, mutant and the CtBPb– e1a mutant, but not with the DCAF7b– e1a mutant (Fig. 2A; Table S1). These results indicate that WT e1a interacts with the protein kinases PRKDC and K6A4S dependent on DCAF7 in addition to DYRK1A, DYRK1B, and HIPK2 (23, 24). Additional key proteins of signaling pathways regulating cell growth that co-IPed with e1a in these analyses include the MAPK signaling pathway kinase ARAF, the TGFβ-signaling pathway-regulated transcription factor SMAD3, and the epidermal growth factor receptor EGFR (Fig. 2B; Table S1).

DCAF10 associates with and destabilizes e1a and regulates IRF3 stability

The most differentially bound protein between WT e1a and all three e1a C-terminal mutants was DCAF10 (aka WDR32), which bound to WT e1a but not the e1a C-terminal mutants in both A549 cells and HBTECs (Table S1; Fig. 3A). DCAF10 was originally identified as a DDB1-interacting WD-repeat-containing protein (42). DDB1 is a central scaffold subunit of a class of cullin 4A and 4B-containing multi-subunit ubiquitin ligases that bind and polyubiquitinylate target proteins by associating with alternative specificity subunits (42). Consequently, DCAF10 may function as a substrate receptor for a CUL4-DDB1 E3 ubiquitin ligase complex (i.e., a Cullin 4-ring ligase or "CRL4") (42). The specific

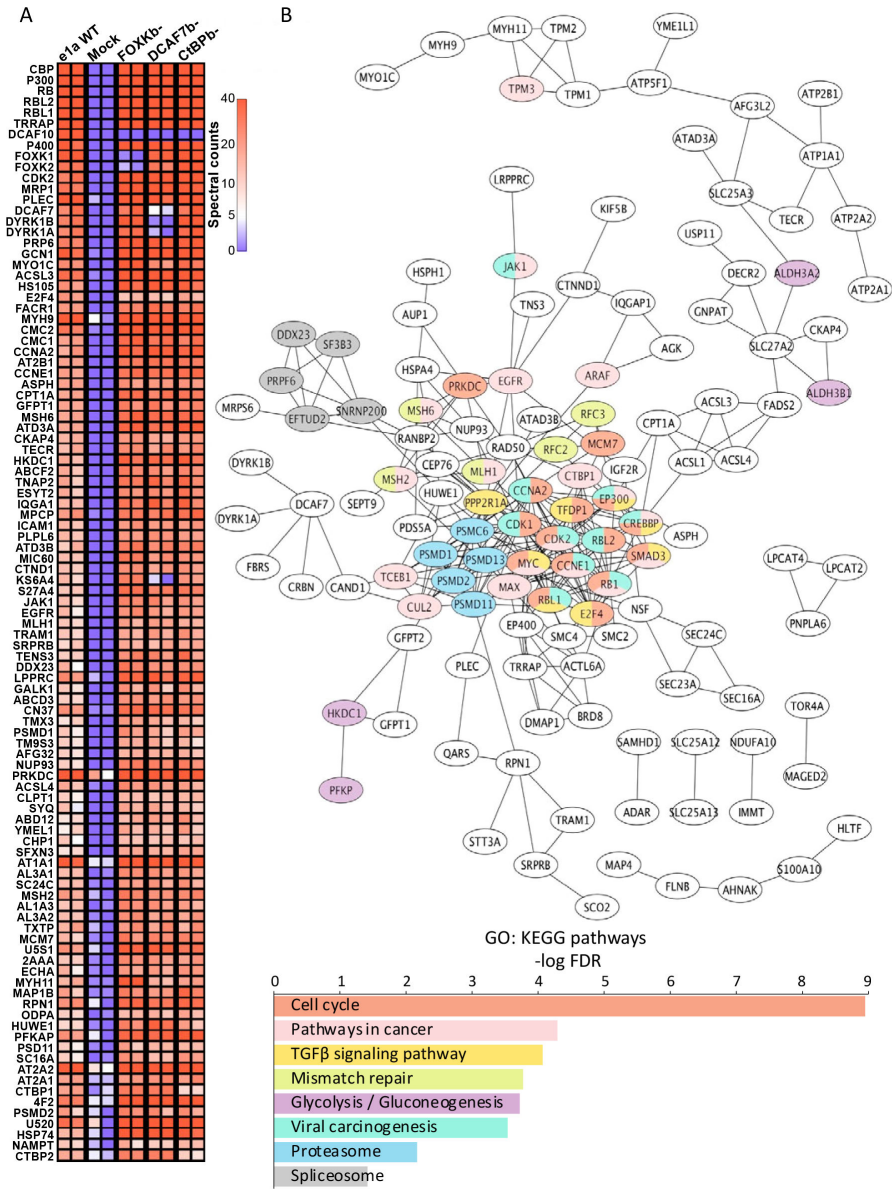

FIG 2 e1a interactome. (A) Heatmap displaying values for spectral counts of peptides from proteins detected by mass spec from M58 (anti-e1a) IPs. Values for duplicate mass spec runs are represented in adjacent columns. The heatmap is limited to proteins with an average of 10 spectral counts or higher between duplicates and ≥5-fold enrichment of WT e1a over mock. (B) Cytoscape protein-protein interaction map for 191 proteins that were enriched for binding to WT e1a and at least two e1a C-terminal mutants >5-fold over mock. Colors refer to the gene ontology shown below. Below, select enriched KEGG pathways gene ontologies for proteins represented in the Cytoscape protein-protein interaction network.

interaction of DCAF10 with WT e1a but not e1a C-terminal mutants was confirmed by e1a IP-western blot from A549 cells infected with the HAdV-C5 vector for HA-tagged DCAF10 (Fig. 3B).

To determine if DCAF10 does, indeed, function as a specificity subunit for a CRL4 ubiquitin ligase, we performed DCAF10 siRNA knock-down (KD) experiments in primary HBTECs, which reduced DCAF10 mRNA to ~30%–40% the level in negative control (siCtrl) transfected cells (Fig. 3C). DCAF10 KD resulted in an increase in WT e1a protein, but no change in the levels of the e1a C-terminal mutant proteins that do not associate with DCAF10 (Fig. 3D). While DCAF10 KD caused e1a protein to increase, it had no effect on e1a mRNA levels (Fig. 3E). These results indicate that DCAF10 association with e1a, either

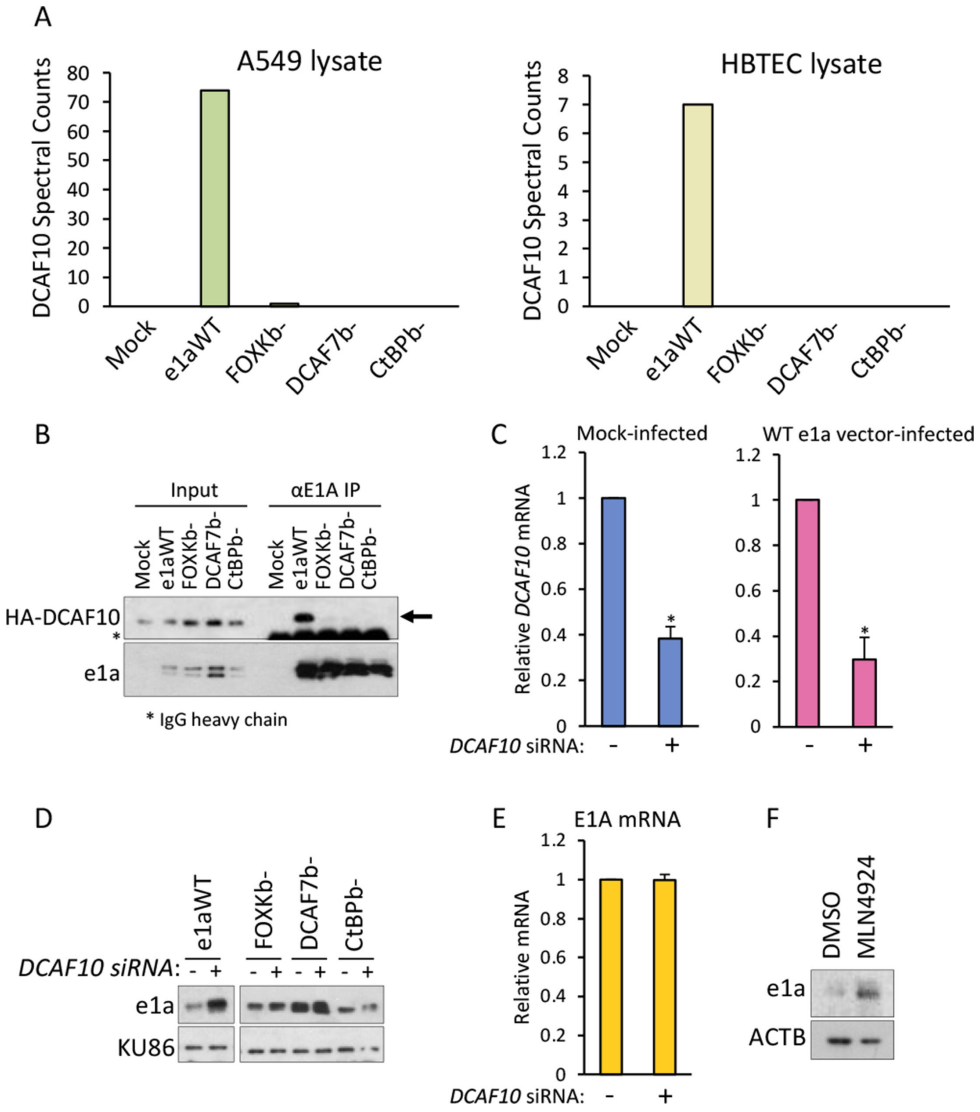

FIG 3 WT e1a binds DCAF10, decreasing e1a stability, but e1a mutants in the C-terminal conserved regions are not destabilized. (A) Spectral counts for DCAF10 mapped peptides from anti-e1a (M58) IP mass spec from A549 (left) and HBTEC (right) 24 hpi with vectors for WT or C-terminal mutant e1as as indicated at the bottom. (B) Western blots for HA-DCAF10 (upper panel) and e1a (lower panel) in input cell extract (left lanes) and IPed proteins (right lanes) following M58 (anti-e1a) IP of protein from A549 cells 24 hpi with vectors for WT e1a or the indicated e1a C-terminal mutants. (C) qRT-PCR with cDNA prepared from HBTECs transfected with control or anti-siRNA for 2 days and then mock-infected (left) or infected with the WT e1a vector (right). (D) Western blots with protein from HBTECs transfected for 2 days with control or anti-DCAF10 siRNA and then infected for 24 h with the vectors for WT or C-terminal mutant e1as indicated at the top. (E) qRT-PCR for E1A mRNA with cDNA prepared from HBTECs transfected for 2 days with control (–) or anti-DCAF10 siRNA (+) and then infected with the e1a WT vector for 24 h. (F) Western blots with protein from HBTECs infected with the e1a WT vector for 24 h and then treated for 6 h with control DMSO or 20 µM MLN4924. In C, D, and E, "–" indicates negative control siRNA (siCtrl). In C and E, data represent averages of three experimental replicates + SD.

directly or indirectly as part of a complex, destabilizes e1a protein. Treatment with MLN4924, a selective inhibitor of the NEDD8-activating enzyme required for the activity of Cullin-based E3 ubiquitin ligases (43), confirmed that e1a degradation depends on ubiquitinylation by a Cullin-based E3 (Fig. 3F).

To determine if DCAF10 regulates IRF3 stability, we performed DCAF10 KD in mock-infected HBTECs and HBTECs infected with the vector for wt e1a and western blotted for IRF3. KD of DCAF10 caused an increase in IRF3 protein in both mock-infected

HBTECs and HBTECs expressing wt e1a (Fig. 4A), without increasing IRF3 mRNA (Fig. 4B). DCAF10 KD also activated OASL and IFIT2 mRNA expression, ISGs induced by the e1a C-terminal mutants, in uninfected HBTECs and HBTECs expressing wt e1a (Fig. 4C), indicating that the increased IRF3 protein was functional for activating ISG transcription. These data suggest that e1a binding to DCAF10 inhibits ISG activation by promoting degradation of IRF3, which counteracts ISG activation as a consequence of e1a inhibition of EP300/CREBBP KAT activity during HAdV infection.

DCAF10 association with e1a promotes assembly of a CRL4 E3 ubiquitin ligase

To identify proteins that interact with DCAF10 that might be substrates of a DCAF10-CRL4, HA-tagged DCAF10 was expressed using an HAdV-C5 expression vector that infects HBTECs efficiently and does not express E1A proteins. Proteins associated with HA-DCAF10 were identified by mass spec of anti-HA IPs prepared under conditions that maintain specific protein-protein interactions (Table S2). CRL4 E3 ubiquitin ligase components DDB1, CUL4A, and CUL4B co-immunoprecipitated with HA-DCAF10 when WT e1a was co-expressed (Fig. 5A and C). Although DDB1 co-IPed with HA-DCAF10 in the absence and presence of WT e1a, subunits CUL4A/B, critical for E3 ubiquitin ligase activity, did not co-IP with DCAF10 in the absence of WT e1a (Fig. 5B). Furthermore, WT e1a bound more CUL4A/B than the C-terminal mutants that do not bind DCAF10 (Fig. S2). These results suggest that WT e1a promotes assembly of an e1a-DCAF10-containing Cullin 4-based E3 ubiquitin ligase complex (an "e1a-DCAF10-CRL4").

Importantly, we did not detect co-IP of IRF3 with HA-DCAF10. This argues against a direct interaction between the two proteins and, therefore, against direct ubiquitinylation of IRF3 by the e1a-DCAF10-CRL4. We did find that HUWE1, a HECT-type E3 ubiquitin ligase also targeted by the HIV Vpr-CRL1 E3 (44), co-IPed specifically with HA-DCAF10,

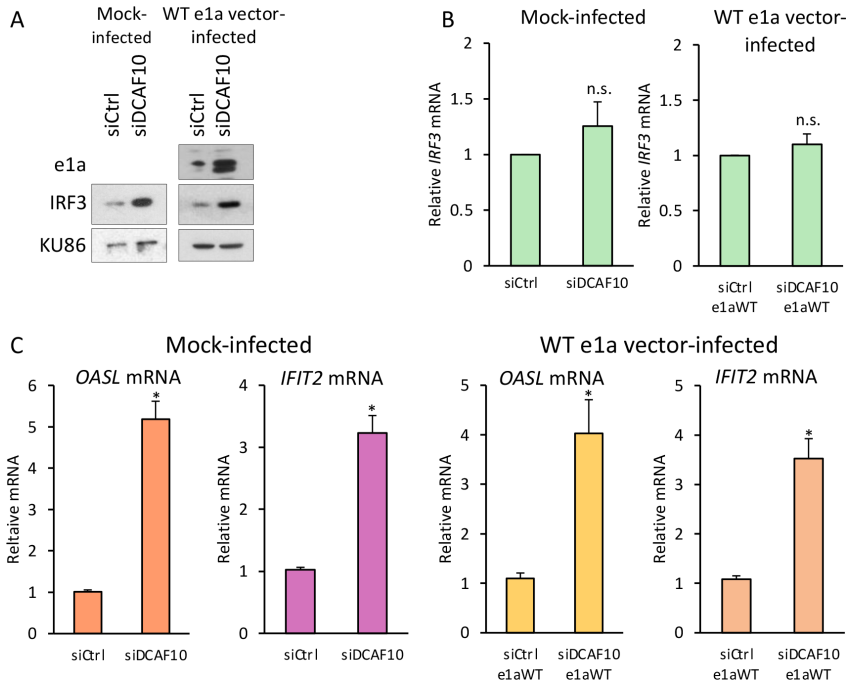

FIG 4 DCAF10 destabilizes IRF3 and inhibits ISG activation. (A) Western blots of protein from HBTECs transfected with control or DCAF10 targeting siRNAs for 2 days, followed by mock-infection or infection with the WT e1a expression vector for 24 h. (B) qRT-PCR with RNA extracted from HBTECs transfected with control or DCAF10 siRNA for 2 days and then 24 h post mock-infection (left) or 24 hpi with the Ad5 vector expressing WT e1a (right). (C) qRT-PCR with RNA extracted from HBTECs treated as in (B). (B, C) Data represent averages of three experimental replicates + SD. "*" indicates $P < 0.01$.

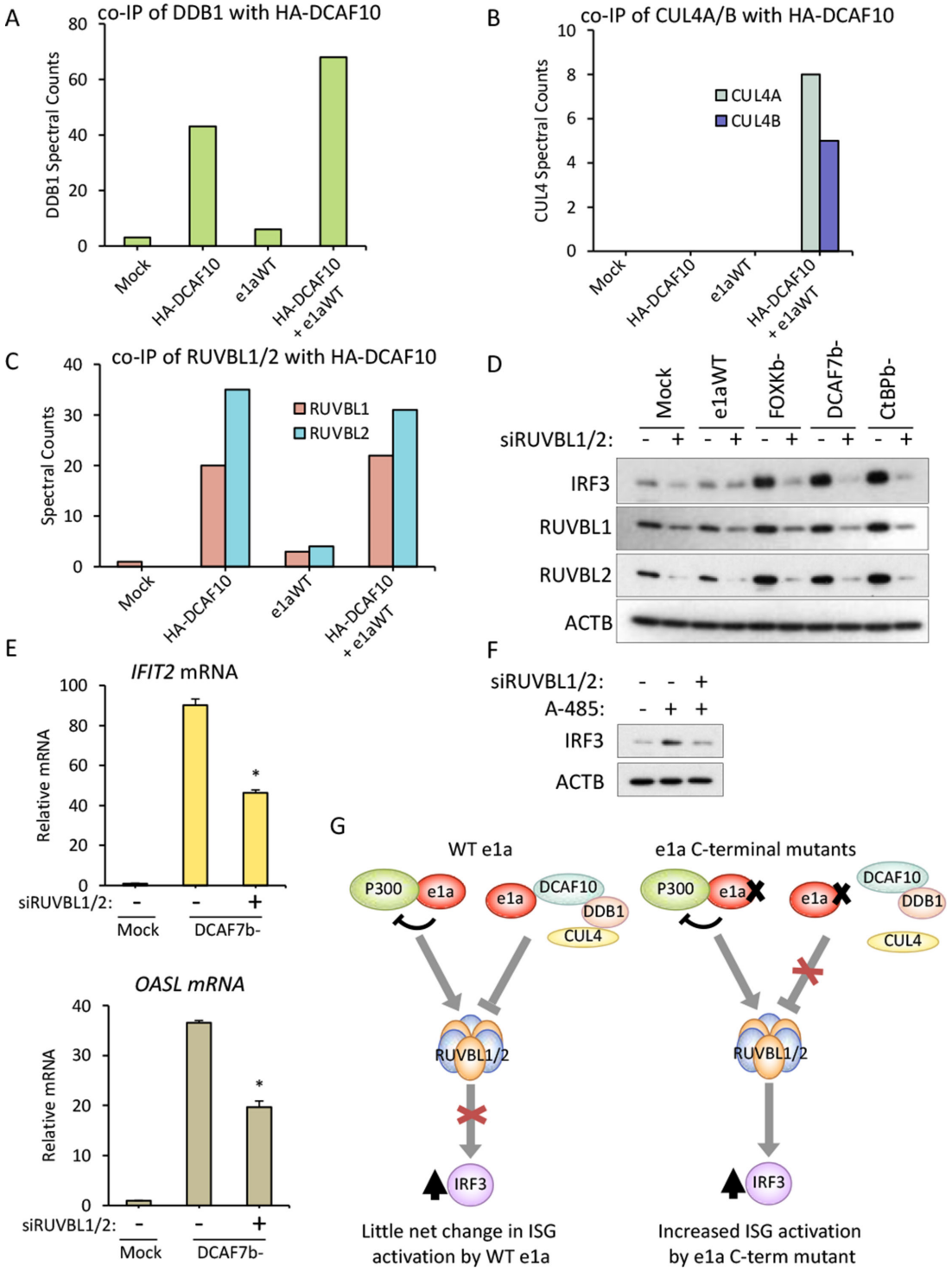

FIG 5 e1a C-terminal mutant stabilization of IRF3 requires RUVBL1/2. Spectral counts of (A) DDB1, (B) RUVBL1/2, (C) CUL4A/B in anti-HA IPs from cells expressing HA-DCAF10. (D) Western blots for the proteins indicated at the left from HBTECs treated for 2 days with control siRNA (–) or siRNAs for RUVBL1 and 2 (+) and then mock-infected or infected with the vectors indicated at the top for 24 h. (E) qRT-PCR of IFIT2 and OASL mRNA from HBTECs treated as in (D). Averages of three experimental replicates + SD. "*" indicates $P < 0.01$ for the difference between control siRNA and RUVBL1/2 siRNA-transfected HBTECs. (F) Western blots for IRF3 or ACTB from HBTECs transfected with control siRNA (–) or siRNAs for RUVBL1/2 (+) for 2 days then treated for 12 h with DMSO or 10 µM A485. (G) Model accounting for the increase in IRF3 protein and ISG activation by the expression of the e1a C-terminal mutants.

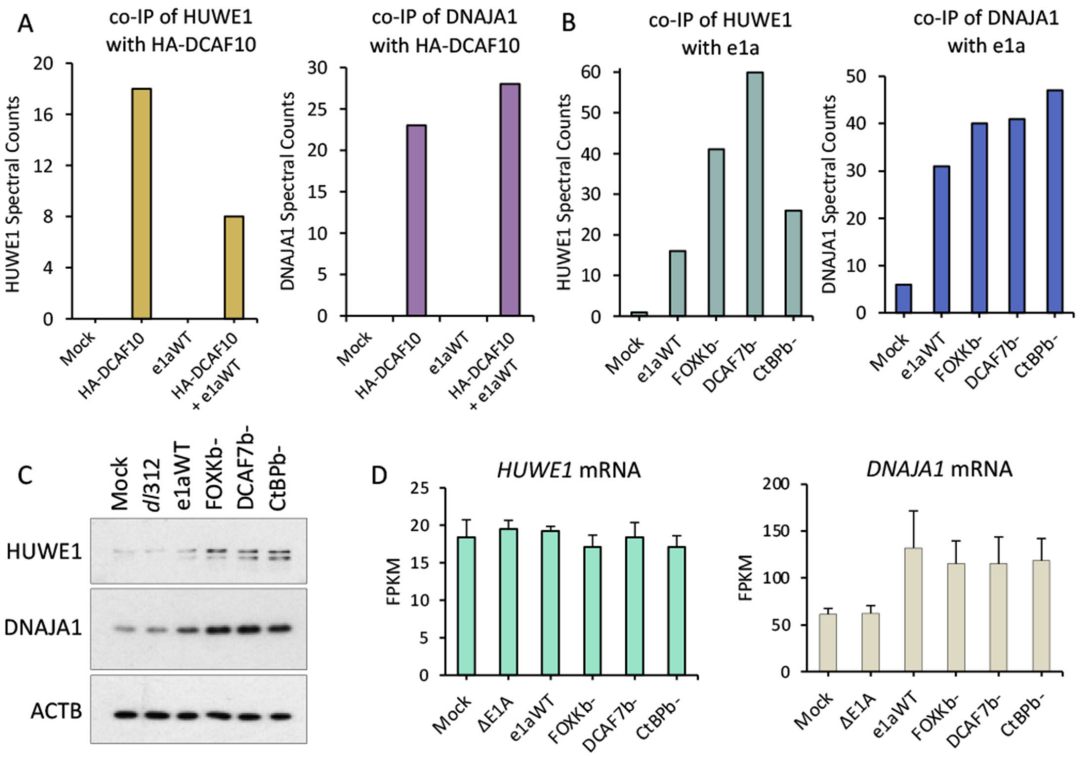

FIG 6 e1a-bound proteins HUWE1 and DNAJA1 accumulate when e1a cannot bind DCAF10. (A) Spectral counts for HUWE1 (left) and DNAJA1 (right) peptides from HA-DCAF10 (anti-HA) IP mass spec from A549 cells 24 hpi. (B) Spectral counts for HUWE1 (left) and DNAJA1 (right) peptides from M58 (anti-e1a) IP mass spec from A549 cells 24 hpi. (C) Western blots with protein from HBTECs 24 hpi with the indicated Ad5 vectors. (D) FPKM of HUWE1 (left) and DNAJA1 (right) from RNA-seq of 24 h-infected HBTECs. Data represent averages of three experimental replicates + SD.

with reduced co-IPed HUWE1 after the expression of e1a (Fig. S3; Fig. 6A). This reduced HUWE1 in the presence of e1a may have been due to enhanced polyubiquitinylation and proteasomal degradation of HUWE1 in the presence of e1a. However, HUWE1 did not appear to be directly involved in regulating IRF3 stability because HUWE1 KD did not alter IRF3 levels in uninfected or e1a C-terminal mutant-expressing HBTECs (data not shown). Other potential specificity subunits that might direct an e1a-Cullin 4A/B-containing ubiquitin ligase to IRF3 or other substrates include ZYG11B and UNC119. Both were specifically IPed by M58 from lysates prepared 24 hpi with the WT e1a vector but not with vectors for the e1a C-terminal mutants (Table S1).

AAA+ ATPases RUVBL1 and RUVBL2 are targets of the e1a-DCAF10-CRL4

The essential AAA+ family ATPases RUVBL1 and RUVBL2 (a.k.a. Pontin and Reptin, respectively) form complexes first studied for their function in DNA damage sensing and repair (34). RUVBL1/2 complexes are also required for maximal transcriptional responses to interferon (32, 33) and to metabolic stress (45). RUVBL1 and RUVBL2 were found in HA-DCAF10 IPs, whether e1a was co-expressed or not (Fig. 5C; Table S2). Unlike HUWE1, KD of both RUVBL1 and RUVBL2 caused a dramatic increase in the level of IRF3 in A485-treated HBTECs (Fig. 5D) with only modest changes in IRF3 mRNA levels (Fig. S4). These results demonstrate that RUVBL1/2 are necessary for stabilization of IRF3 in HBTECs expressing e1a C-terminal mutants. RUVBL1 and RUVBL2 proteins also increased after the expression of the e1a C-terminal mutants but not WT e1a (Fig. 5D), without increases in their mRNAs (Fig. S5), suggesting that DCAF10 regulates the stabilities of RUVBL1/2 as well as IRF3. Importantly for the mechanism of e1a inhibition of innate immunity, RUVBL1/2 KD inhibited activation of ISGs by the e1a C-terminal mutants

(Fig. 5E), possibly because KD of RUVBL1/2 inhibited stabilization of IRF3 by the e1a C-terminal mutants (Fig. 5D).

The results above indicate that RUVBL1/2 are required for e1a C-terminal mutants to stabilize IRF3. To determine if RUVBL1/2 are also necessary for the IRF3 stabilization observed with inhibition of EP300/CBP acetyltransferase activity (Fig. 1G), we treated HBTECs with A485 with or without RUVBL1/2 KD (Fig. 5F). A485 treatment increased IRF3 protein as before, but RUVBL1/2 KD prevented the A485-induced increase (Fig. 5F). Taken together these data suggest that inhibition of EP300 and CBP acetyltransferases by A485 or by the e1a C-terminal mutants leads to stabilization of IRF3 dependent on RUVBL1/2 activity and that the e1a-DCAF10 interaction inhibits RUVBL1/2 from stabilizing IRF3 and activating interferon-stimulated genes (Fig. 5G).

Since our results were consistent with the model that e1a assembles a DCAF10-containing CRL4 E3 ubiquitin ligase complex, we searched for proteins that might be substrates for this complex in the e1a-IPs. HUWE1 and DNAJA1 co-IPed with both e1a and HA-DCAF10 (Fig. 6A and B), raising the hypothesis that they are substrates for the e1a-DCAF10-CRL4 E3 ubiquitin ligase complex. Supporting this hypothesis, western blots for HUWE1 and DNAJA1 from infected HBTECs showed that both proteins had higher levels when e1a C-terminal mutants were expressed compared to WT e1a (Fig. 6C) although their mRNA levels were not higher (Fig. 6D). Additionally, more HUWE1 and DNAJA1 associated with e1a C-terminal mutants compared with WT e1a (Fig. 6B). This could be due to a lower rate of HUWE1 and DNAJA1 degradation when e1a cannot complex with DCAF10. These results are consistent with the model that e1a redirects a DCAF10-CRL4 to target e1a-bound proteins such as HUWE1 and DNAJA1, as well as RUVBL1 and RUVBL2 and other potential substrates, for ubiquitin ligase-mediated proteasomal degradation.

DISCUSSION

Several recent observations have provided clues to the functions of three highly conserved peptides in the ~75 C-terminal amino acids of HAdV-C5 E1A. When expressed as an E1A mutant with a deletion of the entire N-terminal half of E1A, the C-terminal half of E1A binds RUVBL1, an AAA+ ATPase required for maximal activation of genes stimulated by interferons (33). RUVBL1 and RUVBL2 were earlier studied as members of a complex required for the response to metabolic stress (45). Three types of host proteins were found to bind to highly conserved peptides in the C-terminal region of E1A (Fig. S1): An ~25 aa Ser/Thr-rich peptide beginning ~175 aa from the C-terminus of the E1A proteins of the species C respiratory adenoviruses (orange in Fig. S1) binds transcription factors FOXK1 and its closely related paralog FOXK2, dependent on E1A-phosphorylation in this region (22). This region includes the most highly phosphorylated site in both the large and small E1A proteins, S219 (large E1A numbering) (46). A second region near the E1A C-terminus (169—193) binds host protein DCAF7 and its associated protein kinases DYRK1A, DYRK1B, and HIPK2 (24). The first host proteins observed to bind to the region of E1A encoded by the second exon bind near the C-terminus and consequently were named C-terminal-binding proteins 1 and 2 (CtBP1/2) (25). CtBP1/2 are orthologs of a critical co-repressor regulating multiple genes during *Drosophila* embryogenesis (26). Here, we report that the three separate interactions of these peptides in the C-terminal region of E1A with host proteins FOXK1/FOXK2, DCAF7 and its associated protein kinases, and CtBP1/CtBP2 lead to assembly of a ubiquitin ligase complex that targets RUVBL1, RUVBL2, and E1A proteins for proteasomal degradation and indirectly induces IRF3 degradation.

RUVBL1 and RUVBL2 form a complex of two heterohexomeric ring AAA+ ATPases stacked on top of each other into a 12-mer that is required for quaternary complex assembly of several cellular "multiprotein machines" (34). Adenovirus E1A C-terminal mutants defective for binding cellular proteins FOXK1/2, DCAF7, or CtBP1/2 through these three conserved E1A peptides potently activate transcription of ~50 interferon-stimulated genes (ISGs) (21). Activation of these ISGs requires transcription factor IRF3

which is normally regulated by polyubiquitinylation and proteasomal degradation (27, 28). The expression of any one of these three E1A C-terminal mutants causes stabilization of IRF3 which accumulates to high concentration, is transported into nuclei, associates with chromatin, and is phosphorylated at its previously discovered activating sites (47) leading to transcriptional activation of the ~50 ISGs (21). Since infection with the E1A deletion mutant *dl*312 (30) with a nearly complete deletion of E1A does not activate this antiviral response, adenovirus DNA alone does not activate it. This may be because adenovirus DNA is sterically blocked from detection by pathogen-associated molecular pattern receptors (PAMPs) such as TLR9 in endosomes (48) and cyclic GMP-AMP synthase (cGAS) and other sensors of DNA in the cytoplasm (49). This blockage of viral DNA recognition probably results from thousands of copies of the small positively charged histone-like virion protein VII blocking DNA interactions with PAMPs (50, 51). These observations led us to investigate how the expression of E1A mutant proteins, and not adenovirus nucleic acids, triggered this antiviral response, and how this antiviral response was prevented by WT E1A, dependent on these three interactions with different host cell proteins not previously understood to be involved in a common function.

Inhibition of EP300 and CREBBP lysine acetyltransferase activity leads to IRF3 stabilization and activation of ISGs

Experiments with HAdV-C5 vectors expressing E1A double interaction mutants defective for binding both EP300/CREBBP and DCAF7, or RBs and DCAF7, or the TIP60 complex and DCAF7 revealed that E1A C-terminal mutants must bind EP300/CREBBP through their N-terminal regions to trigger IRF3 stabilization (Fig. 1E and F). Also, inhibition of EP300/CREBBP lysine acetyltransferase (KAT) activity with the highly specific small molecule inhibitor A485 (36) was sufficient to induce IRF3 stabilization (Fig. 1G). These results indicate that inhibition of EP300/CREBBP KAT enzymatic activity by either the N-terminal region of E1A or A485 is responsible for triggering this innate immune response. Since EP300/CREBBP are common targets of DNA tumor viruses, e.g., HPV (52), SV40 and mouse polyomavirus large T antigens (53, 54), and adenovirus E1A (14), IRF3 stabilization and activation in response to EP300/CREBBP inhibition may have evolved in metazoans as a generalized antiviral host defense. Since this previously uncharacterized activation of an innate immune response by inhibition of EP300/CREBBP KAT activity was revealed by E1A mutants defective for any one of the three E1A C-terminal protein interactions, and WT E1A prevented IRF3 stabilization, we hypothesize that WT E1A evolved an activity dependent on the three C-terminal interactions in order to retain EP300/CREBBP inhibition but counter the resulting IRF3 stabilization that otherwise induces ISGs and inhibits viral replication (21). Our earlier complementation analysis indicated that a single E1A protein molecule must bind FOXK1/2, the DCAF7-complexes, and CtBP1/2 to prevent activation of ISG expression (21). These results suggest that assembly of a complex containing the N-terminal half of the large or small E1A proteins, and these three seemingly unrelated host proteins prevents IRF3 stabilization that is otherwise induced by E1A inhibition of EP300/CREBBP acetyltransferase activity.

DCAF10 associates with E1A dependent on all three E1A C-terminal interactions with these host cell proteins

To explore why all three of the E1A C-terminal mutants fail to prevent IRF3 stabilization, we searched for proteins differentially bound to WT E1A versus all three of the E1A C-terminal mutants. DCAF10 fulfills these criteria: it associated with WT E1A but none of the three E1A C-terminal mutants (Fig. 3A and B). A possible explanation for why three different, well-separated mutations in E1A's C-terminal region resulted in loss of DCAF10 binding may be because of common alterations in E1A phosphorylation of all three mutants compared to WT E1A. Previously, we reported that WT E1A is phosphorylated resulting in decreased mobility during SDS-PAGE compared to the phosphatase-treated protein (21). However, phosphorylation of the E1A C-terminal mutants does

not occur (21). Phosphorylation of Ser/Thr in the region of E1A bound by FOXK1/2 (orange in Fig. S1) is necessary for the E1A-FOXK1/2 interaction (21). These observations indicate that this region of E1A is a "phospho-degron." Regulation of the phosphorylation of phospho-degron peptides is a strategy commonly used by the cell to regulate protein polyubiquitinylation and proteasomal degradation. Indeed, DCAF10 association destabilized WT E1A (Fig. 3D). The lack of a mobility shift during SDS-PAGE for all three C-terminal mutants suggests that E1A phosphorylation at a specific site(s) is required for DCAF10-binding to E1A and that E1A polyubiquitinylation and proteasomal degradation is decreased for all three of the E1A C-terminal mutants because they fail to be phosphorylated. One or more of the DCAF7 associated protein kinases DYRK1A, DYRK1B, HIPK2 (24), or KS6A4 (identified here, Fig. 2A; Table S1) may phosphorylate these sites in E1A, stimulating FOXK1/2 binding and assembly of the complete E1A-DCAF10-CRL4 ubiquitin ligase complex.

E1A-DCAF10 targeting RUVBL1/2 prevents IRF3 stabilization and activation of ISGs in response to EP300/CREBBP inhibition

We did not detect a direct interaction between epitope-tagged HA-DCAF10 and IRF3 in the presence or absence of E1A (Table S2). This suggests that IRF3 is not directly polyubiquitinylated by an E1A-DCAF10-CRL4 E3. However, we did detect association of epitope-tagged DCAF10 with RUVBL1 and RUVBL2 (Fig. 5C). Stabilization of RUVBL1/2 by the E1A C-terminal mutants also was observed, and RUVBL1/2 were required for stabilization of IRF3 by the E1A C-terminal mutants (Fig. 5D). Since the E1A C-terminal mutants caused an increase in RUVBL1/2 proteins but not their mRNAs (Fig. 5D; Fig. S5), they likely cause stabilization of RUVBL1 and RUVBL2 proteins. In contrast, WT E1A prevented RUVBL1/2 stabilization (Fig. 5D). Although DCAF10 fulfills many of the requirements of a substrate specificity factor that targets the postulated E1A-CRL4 ubiquitin ligase to IRF3, ZY11B (Table S1) (gene symbol ZYG11B) and U119A (Table S1) (gene symbol UNC119) may be redundant substrate specificity subunits with overlapping specificity to DCAF10 because they also fail to bind to all three of the C-terminal mutants. ZYG11B is an established specificity factor for one of the ubiquitin ligases that enforce the "N-end rule" inducing degradation of polypeptides beginning with N-terminal glycine (55). UNC119 is itself an N-terminal myristoylated protein found in basal bodies of primary cilia that is required for cilia assembly and function (56). The biochemical activity of UNC119 that controls cilia assembly is not known. Our finding that UNC119 is associated with an E1A-containing ubiquitin ligase complex suggests that UNC119 may function in cilia as a specificity subunit of a ubiquitin ligase.

Detection of higher levels of DDB1 and CUL4A and B binding to HA-DCAF10 in the presence of E1A (Fig. 5A and C) suggests that E1A promotes assembly of an E1A-CRL4 complex. Also, the stabilization of WT E1A by knocking-down DCAF10, but not by knocking-down DCAF10 in cells expressing the E1A C-terminal mutants unable to bind DCAF10 (Fig. 3D), suggests that DCAF10 binds to WT E1A as part of an active ubiquitin ligase complex that polyubiquitinylates WT E1A as well as other proteins associated with WT E1A including RUVBL1 and RUVBL2. Our observations that E1A-bound proteins HUWE1 and DNAJA1 (Table S1) accumulated to higher levels when E1A had mutations blocking its interaction with DCAF10 (Fig. 6C) are consistent with this model that E1A directs substrate targeting by this DCAF10-containing CRL4 ubiquitin ligase to proteins associated with E1A.

A similar activity to the one we propose here for the C-terminal region of E1A was first discovered for the HIV-1 Vpr protein (57). Like the E1A association with DCAF10, Vpr binds DCAF1 and forms a DDB1-CRL4 E3 ubiquitin ligase that polyubiquitinylates several cellular proteins that inhibit HIV replication (57).

A surprising observation was that RUVBL1/2 knock-down prevented the increase in IRF3 by the expression of the E1A C-terminal mutants and by inhibition of EP300/CREBBP KAT activity with A485 (Fig. 5D and F). IRF3 stabilization was presumably due to inhibition of IRF3 polyubiquitinylation following the expression of the E1A C-terminal mutants or

treatment with A485. Also, Olanubi et al. (33) reported that the E1A C-terminal half binds RUVBL1 thereby inhibiting ISG activation by IFNα. These observations might be explained if the RUVBL1/2 dodecamer is required for the proper folding and stabilization of IRF3. Alternatively, RUVBL1/2 may be required to cause a conformational change in IRF3 that reveals a site of polyubiquitinylation.

RUVBL1/2 function in both the cytoplasm and nucleus as dodecameric HSP90 co-chaperones consisting of two stacked heterohexameric ring AAA+ ATPases (34). In the cytoplasm, RUVBL1/2-containing complexes function in the assembly of several essential multi-molecular complexes such as snRNPs, snoRNPs, the telomerase RNP, RNA polymerases II and III, and the PIKK family of multi-subunit protein kinases (34). The PIKK family includes mTORC1, which regulates ribosome and protein synthesis (58), and SMG-1 required for nonsense-mediated mRNA decay (NMD) (58). In the nucleus, RUVBL1/2 regulate transcription, DNA double-strand break repair, and cell size as subunits of chromatin remodeling complexes TIP60 and INO80 (18, 19), the Fanconi Anemia DNA repair complex (59), and MYC-containing complexes (60). We speculate that the connection between RUVBL1/2 and IRF3 polyubiquitinylation is mediated by a chaperone-like complex similar to R2TP, a subcomplex in several multi-protein chaperone complexes consisting of RUVBL1, RUVBL2, PIH1D1, and RPAP3 (34). RUVBL1, RUVBL2, and RPAP3 were enriched in anti-HA IPs from cells expressing HA-DCAF10, but not PIH1D1 (Table S2). The modular nature of these complexes suggests that another subunit may substitute for PIH1D1 in a complex similar to R2TP that binds WT E1A.

In addition to the DCAF10-E1A ubiquitin ligase targeting IRF3 discussed above assembled by the C-terminal region of E1A, earlier studies established the importance of the E1B-55K/E4orf6 ubiquitin ligase during viral infection of permissive human cells (61). The virus-encoded E1B-55K and E4orf6 proteins form a complex that polyubiquitinylates p53 and a subunit of the MRN complex, leading to their proteosomal degradation. If the MRN complex is not inactivated, it causes Ad5 genomes to be ligated together in random orientation, interfering with viral DNA replication and packaging.

AAA+ ATPases such as RUVBL1/2 are the "moving parts" of several cellular multi-protein machines such as myosins. They undergo large conformational changes when ATP is exchanged for ADP in their nucleotide binding pocket, when that ATP is hydrolyzed to ADP and phosphate, and again when the phosphate is released. Such large, regulated changes in protein conformation in RUVBL1/2 and HSP90-associated proteins bound to RUVBL1/2, including IRF3, may be necessary to expose sites in the target proteins to ubiquitin ligases. Whatever the molecular mechanism, it is clear from the results reported here that RUVBL1/2 are required to activate innate immunity in response to inhibition of EP300/CREBBP KAT activity (Fig. 5E and F). Since abnormally high IRF3 activity appears to contribute to the pathology of several auto-immune diseases, it is important to pursue additional studies that explain why the RUVBL1/2 AAA+ ATPases are required for stabilization of IRF3 when EP300/CREBBP KAT activity is inhibited. Understanding RUVBL1/2 function in the regulation of IRF3 activity may allow rational design of therapeutic approaches to reduce IRF3 activity and reduce pathology in many auto-immune diseases.

MATERIALS AND METHODS

siRNA and small-molecule treatment

siRNA KD was performed in HBTECs using Invitrogen RNAiMAX reverse transfection protocol. Cells were plated in antibiotic free HBTECs media containing indicated Ambion/ThermoFisher Silencer Select siRNA for a final concentration of 10 nM that was pre-incubated in 7.5 µL of lipofectamine RNAiMAX (ThermoFisher Cat#13778075) reagent in 750 µL of Opti-MEM in 6 cm^2 plates. For a complete list of Ambion/ThermoFisher Silencer Select siRNAs used see Table 1. Ambion/ThermoFisher Silencer Negative Control no.1 AM4611 was used as a negative control (siCtrl). Double knock-downs were performed with a total siRNA concentration of 10 nM. MLN4924 (BostonBiochem Cat# I-502) was

TABLE 1 siRNA targets

siRNA target	Ambion siRNA ID #	siRNA sequence
IRF3	s7507	ACACCUCUCCGGACACCAAtt
DCAF10	s35727	CUCUACGACUGACUCAUUAtt
RUVBL1	s16369	CGAGUGAUGAUAAUCCGGAtt
RUVBL2	s21309	GAAACGCAAGGGUACAGAAtt

added directly to media of cultured HBTECs at a final concentration of 20 µM for a treatment time of 6 h. A485 (MedChemExpress Cat# HY-107455) was added directly to media of cultured HBTECs at a final concentration of 10 µM for a treatment time of 12 h. DMSO was used as a negative control for both MLN4924 and A485 at an equal volume.

Western blot

Proteins were extracted from indicated cells by lysis in EBC (120 mM NaCl, 0.5% NP-40, 50 mM Tris-Cl pH 8.0, and Roche cOmplete protease inhibitors Cat#04693132001). Protein concentration was quantified by Bradford assay, normalized in Laemmli buffer, heated for 10 min at 65°C, and then resolved in a 9% SDS-polyacrylamide gel. Proteins were electrotransferred to a polyvinylidene difluoride (PVDF) membrane and then blocked in 5% milk in TBS-Tween 0.1% (blocking buffer) for 30 min. Primary antibody M58 (anti-E1A), M73 (anti-E1A), H3K27ac, H3, KU-86 (H-300), β-Actin, IRF3, RUVBL1, RUVBL2, HUWE1, or DNAJA1 (Table 2) was added at 1:2,000 dilution or 1:200 for M58 and M73 hybridoma supernatant for 1 h at room temperature or O/N at 4°C. Membranes were washed 3× in TBS-Tween (0.1%), and then HRP-conjugated anti-mouse or anti-rabbit secondary antibodies were added for 1 h room temperature in blocking buffer. Membranes were then washed 3× in TBS-Tween (0.1%) prior to addition of ECL reagent for the detection of chemiluminescence. Western blots were validated with replicates of two or more with representative western blots presented.

qRT-PCR

Cells were collected at indicated times following transfection, and RNA was isolated using QIAGEN RNeasy Plus Mini Kit (Cat#74134). One microgram of RNA, as measured

TABLE 2 Antibodies

Antibody	Source	Identifier
Rabbit polyclonal antiH3K27ac	Active Motif	Cat#39133; RRID: AB_2561016; Lot#31814008
Mouse monoclonal anti-E1A (M58) hybridoma supernatant	Produced in house	(38)
Rabbit polyclonal antiBeta-Actin	GeneTex	Cat#GTX16039; RRID: AB_367276
Rabbit polyclonal antiKU-86 (H-300)	Santa Cruz	Cat#sc-9034; RRID: AB_2218743
Rabbit monoclonal antiIRF3 (D6I4C)	Cell Signaling Technology	Cat#11904S
Mouse monoclonal antiH3	Abcam	Cat#ab10799
Anti-HA Tag (C29F4)	Cell Signaling Technology	Cat#3724S
Rabbit monoclonal anti-Pontin/RUVBL1 (D1L8J)	Cell Signaling Technology	Cat#74775S
Rabbit monoclonal anti-Reptin/RUVBL2 (D8N3J)	Cell Signaling Technology	Cat#12668S
Rabbit polyclonal anti-HUWE1	Bethyl	Cat#A300-486A
Rabbit polyclonal anti-DNAJA1	Bethyl	Cat#A304-516A

TABLE 3 Primers

Primer target	Primer sequence
OASL Forward	5′ CAACGTGGCAGAAGGGTACA 3′
OASL Reverse	5′ TCAAGTGGATGTCTCGTGCC 3′
IFIT2 Forward	5′ CCTGCCGAACAGCTGAGAA 3′
IFIT2 Reverse	5′ TAGTTGCCGTAGGCTGCTCT 3′
MX1 Forward	5′ AGCTCGGCAACAGACTCTTC 3′
MX1 Reverse	5′ CCGTACGTCTGGAGCATGAA
IRF3 Forward	5′ GCCCCGACCTTCCATCG 3′
IRF3 Reverse	5′ CAGTTGCCCCAGGTCCAG 3′
DCAF10 Forward	5′ TTTCGCACCATGACTAGCCT 3′
DCAF10 Reverse	5′ CACAAGCAACTGTCAGCACT 3′
E1A Forward	5′ CCACCTACCCTTCACGAACT 3′
E1A Reverse	5′ AAAATCTGCGAAACCGCCTC 3′

by Qubit fluorometer, was used for reverse transcription with SuperScript III FirstStrand Synthesis SuperMix using random hexamer primers (Table 3). qRT-PCR was performed with 5 µL of cDNA, diluted 1:10. Runs were done using an ABI 7500 Real Time Thermocycler and reactions took place in optical-grade, 96-well plates (Applied Biosystems, Carlsbad, CA, USA) 25 µL total volume with primers at a concentration of 900 nM and 12.5 µL of 2× FastStart Universal SYBR Green Master (Rox) (Roche Cat#04913850001). Relative mRNA levels were calculated as $2^{\Delta Ct}$. Equal cDNA loading was confirmed with primers to 18 s rRNA cDNA. Data are presented as an average of 3 or more biological replicates ± SD.

RNA-seq procedure and data analysis

Previously published RNA-seq data used in this study can be downloaded from GEO accession GSE105039. 1×10^6 Low-passage HBTEC were mock-infected or infected with Ad5 E1A-E1B substituted, E3-deleted vectors expressing WT Ad2 small E1A proteins from the dl1520 deletion removing the 13S E1A mRNA 5′ splice site (3) 3 days after reaching confluence. RNA was isolated 24 hpi using QIAGEN RNeasy Plus Mini Kit. Eluted RNA was treated with Ambion DNA-free DNA Removal Kit and then Ambion TRIzol reagent, precipitated with isopropanol, and dissolved in sterile water. RNA concentration was measured with a Qubit fluorometer. One microgram of RNA was fragmented and copied into DNA and then PCR amplified with bar-coded primers for separate samples to prepare sequencing libraries using the Illumina TruSeq RNA Sample Preparation procedure. Libraries were sequenced using the Illumina Hiseq-2000 to obtain single end 50 base pair reads. Sequences were aligned to the hg19 human genome sequence using TopHat v2. FPKM (fragments per kb per million mapped reads) for each annotated hg19 RefSeq gene ID was determined using Cuffdiff v2 from Cufflinks RNA-Seq analysis tools at http://cufflinks.cbcb.umd.edu.

Co-immunoprecipitation

Co-IPs were performed using M58 crosslinked to protein G agarose beads or with goat anti-HA agarose immobilized (Bethyl cat#S190-138). One milliliter of clarified M58 hybridoma supernatant was incubated with 50 µL of 50% slurry protein G agarose beads on nutator for 4 h at 4°C. Beads were washed 3× with 0.2 M sodium borate pH 9, and then antibody was crosslinked to protein G beads in 20 mM DMP in 0.2 M sodium borate pH 9 for 40 min on nutator at room temperature. Beads were then washed once with 0.2 M ethanolamine pH 8 and then quenched in 1 mL ethanolamine pH 8 on nutator for 2 h at room temperature. To remove uncoupled IgGs, beads were washed 3× with 0.58% acetic acid and 150 mM NaCl and then washed 3× with PBS. Cells were lysed in EBC lysis buffer (120 mM NaCl, 0.5% NP-40, 50 mM Tris-Cl pH 8.0, and Roche cOmplete protease

inhibitors and phosphatase inhibitors Sigma Aldrich cat# P5726-1ML and P0044-1ML) on ice. For western blots, 2–4 mg of protein in supernatant lysate was precleared with 30 µL agarose G beads for 1 h and then immunoprecipitated overnight at 4°C with M58 cross-linked to agarose G beads. Immuno-bead complexes were washed three times with cold EBC buffer, eluted in Laemmli buffer, and incubated 10 min at 65°C. For mass spec samples, 5–6 mg of protein in supernatant lysate was precleared with 50 µL agarose G beads for 1 h, and then 50 µL of M58-beads or anti-HA beads was added for 4 h at 4°C for immunoprecipitation. Immuno-bead complexes were washed four times with cold PBS and then eluted in 500 µL of 0.2 M glycine pH 2.0. Proteins in 400 µL of eluent were precipitated with 20% TCA on ice for 1 h and then microcentrifuged at 14 K rpm for 25 min at 4°C. Supernatant was removed, and pellets were washed with 500 µL of ice cold acetone and then microcentrifuged at 14 K rpm for 25 min at 4°C. Supernatant was removed, and pellets were stored in parafilmed tubes at −20°C for eventual trypsin digest and mass spec.

Sample digestion and desalting

The protein pellets were resuspended in digestion buffer (8 M urea, 100 mM Tris pH 8.5), later reduced and alkylated via sequential 20 min incubations of 5 mM TCEP 10 mM iodoacetamide at room temperature in the dark while being mixed at 1,200 rpm in an Eppendorf thermomixer. Then, the proteins were digested by 0.1 µg of Lys-C (Thermo Scientific, 90051) and 0.8 µg Trypsin (Thermo Scientific, 90057) proteases at 37°C overnight. The digested samples were quenched by the addition of formic acid to 5% (vol/vol) final concentration. Each sample was desalted via C18 stage tips (Thermo Scientific, 87784), washed twice in 200 µL of 5% formic acid, and eluted in 60% Acetonitrile with 5% formic acid. Eluted peptide samples were dried in a SpeedVac before being resuspended in 5% formic acid.

LC-MS acquisition

Peptide samples were separated on a 75 µM ID, 25 cm C18 column packed with 1.9 µM C18 particles (Dr. Maisch GmbH HPLC) using a 140 min gradient of increasing acetonitrile and eluted directly into a Thermo Orbitrap Fusion Lumos instrument where MS/MS spectra were acquired by Data Dependent Acquisition (DDA).

Mass spectrometry analysis

Analysis was performed by using ProLuCID (62) and DTASelect2 (63) implemented in Integrated Proteomics Pipeline IP2 (Integrated Proteomics Applications). Protein and peptide identifications were filtered using DTASelect and required a minimum of two unique peptides per protein and a peptide-level false positive rate of less than 1% as estimated by a target-decoy database competition strategy.

AUTHOR AFFILIATIONS

[1]Molecular Biology Institute, University of California, Los Angeles, California, USA
[2]Department of Cellular and Molecular Medicine, UCSD School of Medicine, La Jolla, California, USA
[3]Department of Microbiology, Immunology, and Molecular Genetics, University of California, Los Angeles, California, USA
[4]Department of Biological Chemistry, David Geffen School of Medicine at UCLA, Los Angeles, California, USA
[5]Thermo Fisher Scientific, San Jose, California, USA
[6]Department of Biochemistry and Molecular Medicine and the Norris Comprehensive Cancer Center, Keck School of Medicine, USC, Los Angeles, California, USA

AUTHOR ORCIDs

Nathan R. Zemke http://orcid.org/0000-0002-6326-5925
Emily Hsu http://orcid.org/0000-0001-5096-0745

AUTHOR CONTRIBUTIONS

Nathan R. Zemke, Conceptualization, Formal analysis, Funding acquisition, Investigation, Writing – original draft, Writing – review and editing | Emily Hsu, Data curation, Formal analysis, Writing – original draft, Writing – review and editing | William D. Barshop, Formal analysis, Investigation | Jihui Sha, Investigation | James A. Wohlschlegel, Funding acquisition, Investigation, Resources, Supervision.

ADDITIONAL FILES

The following material is available online.

Supplemental Material

Supplemental material (JVI00993-23-s0001.pdf). Supplemental methods and Fig. S1 to S5.
Table S1 (JVI00993-23-s0002.xlsx). e1a IP MS normalized spectral counts.
Table S2 (JVI00993-23-s0003.xlsx). HA DCAF10 IP MS normalized spectral counts.

REFERENCES

1. Reich N, Pine R, Levy D, Darnell JE. 1988. Transcription of interferon-stimulated genes is induced by adenovirus particles but is suppressed by E1A gene products. J Virol 62:114–119. https://doi.org/10.1128/JVI.62.1.114-119.1988
2. Zhao H, Granberg F, Elfineh L, Pettersson U, Svensson C. 2003. Strategic attack on host cell gene expression during adenovirus infection. J Virol 77:11006–11015. https://doi.org/10.1128/jvi.77.20.11006-11015.2003
3. Montell C, Courtois G, Eng C, Berk A. 1984. Complete transformation by adenovirus 2 requires both E1A proteins. Cell 36:951–961. https://doi.org/10.1016/0092-8674(84)90045-x
4. Spindler KR, Eng CY, Berk AJ. 1985. An adenovirus early region 1A protein is required for maximal viral DNA replication in growth-arrested human cells. J Virol 53:742–750. https://doi.org/10.1128/JVI.53.3.742-750.1985
5. Stabel S, Argos P, Philipson L. 1985. The release of growth arrest by microinjection of adenovirus E1A DNA. EMBO J 4:2329–2336. https://doi.org/10.1002/j.1460-2075.1985.tb03934.x
6. Nevins JR, Ginsberg HS, Blanchard JM, Wilson MC, Darnell JE. 1979. Regulation of the primary expression of the early adenovirus transcription units. J Virol 32:727–733. https://doi.org/10.1128/JVI.32.3.727-733.1979
7. Perricaudet M, Akusjärvi G, Virtanen A, Pettersson U. 1979. Structure of two spliced mRNAs from the transforming region of human subgroup C adenoviruses. Nature 281:694–696. https://doi.org/10.1038/281694a0
8. Winberg G, Shenk T. 1984. Dissection of overlapping functions within the adenovirus type 5 E1A gene. EMBO J 3:1907–1912. https://doi.org/10.1002/j.1460-2075.1984.tb02066.x
9. Ruley HE. 1983. Adenovirus early region 1A enables viral and cellular transforming genes to transform primary cells in culture. Nature 304:602–606. https://doi.org/10.1038/304602a0
10. Branton PE, Bayley ST, Graham FL. 1985. Transformation by human adenoviruses. Biochim Biophys Acta 780:67–94. https://doi.org/10.1016/0304-419x(84)90007-6
11. Debbas M, White E. 1993. Wild-type p53 mediates apoptosis by E1A, which is inhibited by E1B. Genes Dev 7:546–554. https://doi.org/10.1101/gad.7.4.546
12. Whyte P, Buchkovich KJ, Horowitz JM, Friend SH, Raybuck M, Weinberg RA, Harlow E. 1988. Association between an oncogene and an anti-oncogene: the adenovirus E1A proteins bind to the retinoblastoma gene product. Nature 334:124–129. https://doi.org/10.1038/334124a0
13. Liu X, Marmorstein R. 2007. Structure of the retinoblastoma protein bound to adenovirus E1A reveals the molecular basis for viral oncoprotein inactivation of a tumor suppressor. Genes Dev 21:2711–2716. https://doi.org/10.1101/gad.1590607
14. Ferreon JC, Martinez-Yamout MA, Dyson HJ, Wright PE. 2009. Structural basis for subversion of cellular control mechanisms by the adenoviral E1A oncoprotein. Proc Natl Acad Sci U S A 106:13260–13265. https://doi.org/10.1073/pnas.0906770106
15. Helin K, Harlow E, Fattaey A. 1993. Inhibition of E2F-1 transactivation by direct binding of the retinoblastoma protein. Mol Cell Biol 13:6501–6508. https://doi.org/10.1128/mcb.13.10.6501-6508.1993
16. Ferrari R, Gou D, Jawdekar G, Johnson SA, Nava M, Su T, Yousef AF, Zemke NR, Pellegrini M, Kurdistani SK, Berk AJ. 2014. Adenovirus small E1A employs the lysine acetylases p300/CBP and tumor suppressor rb to repress select host genes and promote productive virus infection. Cell Host Microbe 16:663–676. https://doi.org/10.1016/j.chom.2014.10.004
17. Fuchs M, Gerber J, Drapkin R, Sif S, Ikura T, Ogryzko V, Lane WS, Nakatani Y, Livingston DM. 2001. The p400 complex is an essential E1A transformation target. Cell 106:297–307. https://doi.org/10.1016/s0092-8674(01)00450-0
18. Squatrito M, Gorrini C, Amati B. 2006. Tip60 in DNA damage response and growth control: many tricks in one HAT. Trends Cell Biol 16:433–442. https://doi.org/10.1016/j.tcb.2006.07.007
19. Sapountzi V, Logan IR, Robson CN. 2006. Cellular functions of TIP60. Int J Biochem Cell Biol 38:1496–1509. https://doi.org/10.1016/j.biocel.2006.03.003
20. Avvakumov N, Kajon AE, Hoeben RC, Mymryk JS. 2004. Comprehensive sequence analysis of the E1A proteins of human and simian adenoviruses. Virology 329:477–492. https://doi.org/10.1016/j.virol.2004.08.007
21. Zemke NR, Berk AJ. 2017. The adenovirus E1A C terminus suppresses a delayed antiviral response and modulates RAS signaling. Cell Host Microbe 22:789–800. https://doi.org/10.1016/j.chom.2017.11.008
22. Komorek J, Kuppuswamy M, Subramanian T, Vijayalingam S, Lomonosova E, Zhao L-J, Mymryk JS, Schmitt K, Chinnadurai G. 2010. Adenovirus type 5 E1A and E6 proteins of low-risk cutaneous beta-human papillomaviruses suppress cell transformation through interaction with FOXK1/K2 transcription factors. J Virol 84:2719–2731. https://doi.org/10.1128/JVI.02119-09
23. Cohen MJ, Yousef AF, Massimi P, Fonseca GJ, Todorovic B, Pelka P, Turnell AS, Banks L, Mymryk JS. 2013. Dissection of the C-terminal region of E1A redefines the roles of CtBP and other cellular targets in oncogenic

transformation. J Virol 87:10348–10355. https://doi.org/10.1128/JVI.00786-13
24. Glenewinkel F, Cohen MJ, King CR, Kaspar S, Bamberg-Lemper S, Mymryk JS, Becker W. 2016. The adaptor protein DCAF7 mediates the interaction of the adenovirus E1A oncoprotein with the protein kinases DYRK1A and HIPK2. Sci Rep 6:28241. https://doi.org/10.1038/srep28241
25. Schaeper U, Boyd JM, Verma S, Uhlmann E, Subramanian T, Chinnadurai G. 1995. Molecular cloning and characterization of a cellular phosphoprotein that interacts with a conserved C-terminal domain of adenovirus E1A involved in negative modulation of oncogenic transformation. Proc Natl Acad Sci U S A 92:10467–10471. https://doi.org/10.1073/pnas.92.23.10467
26. Nibu Y, Zhang H, Levine M. 1998. Interaction of short-range repressors with drosophila CtBP in the embryo. Science 280:101–104. https://doi.org/10.1126/science.280.5360.101
27. Negishi H, Taniguchi T, Yanai H. 2018. The interferon (IFN) class of cytokines and the IFN regulatory factor (IRF) transcription factor family. Cold Spring Harb Perspect Biol 10:a028423. https://doi.org/10.1101/cshperspect.a028423
28. Ikushima H, Negishi H, Taniguchi T. 2013. The IRF family transcription factors at the interface of innate and adaptive immune responses. Cold Spring Harb Symp Quant Biol 78:105–116. https://doi.org/10.1101/sqb.2013.78.020321
29. Cheon H, Stark GR. 2009. Unphosphorylated STAT1 prolongs the expression of interferon-induced immune regulatory genes. Proc Natl Acad Sci U S A 106:9373–9378. https://doi.org/10.1073/pnas.0903487106
30. Jones N, Shenk T. 1979. Isolation of adenovirus type 5 host range deletion mutants defective for transformation of rat embryo cells. Cell 17:683–689. https://doi.org/10.1016/0092-8674(79)90275-7
31. Greber UF, Flatt JW. 2019. Adenovirus entry: from infection to immunity. Annu Rev Virol 6:177–197. https://doi.org/10.1146/annurev-virology-092818-015550
32. Gnatovskiy L, Mita P, Levy DE. 2013. The human RVB complex is required for efficient transcription of type I interferon-stimulated genes. Mol Cell Biol 33:3817–3825. https://doi.org/10.1128/MCB.01562-12
33. Olanubi O, Frost JR, Radko S, Pelka P, Banks L. 2017. Suppression of type I interferon signaling by E1A via RuvBL1/Pontin. J Virol 91:e02484-16. https://doi.org/10.1128/JVI.02484-16
34. Dauden MI, López-Perrote A, Llorca O. 2021. RUVBL1-RUVBL2 AAA-ATPase: a versatile scaffold for multiple complexes and functions. Curr Opin Struct Biol 67:78–85. https://doi.org/10.1016/j.sbi.2020.08.010
35. Hardy S, Kitamura M, Harris-Stansil T, Dai Y, Phipps ML. 1997. Construction of adenovirus vectors through cre-lox recombination. J Virol 71:1842–1849. https://doi.org/10.1128/JVI.71.3.1842-1849.1997
36. Lasko LM, Jakob CG, Edalji RP, Qiu W, Montgomery D, Digiammarino EL, Hansen TM, Risi RM, Frey R, ManavesV, et al. 2018. Author correction: discovery of a selective catalytic p300/CBP inhibitor that targets lineage-specific tumours. Nature 558:E1. https://doi.org/10.1038/s41586-018-0111-5
37. Lieber M, Smith B, Szakal A, Nelson-Rees W, Todaro G. 1976. A continuous tumor-cell line from a human lung carcinoma with properties of type II alveolar epithelial cells. Int J Cancer 17:62–70. https://doi.org/10.1002/ijc.2910170110
38. Harlow E, Franza BR, Schley C. 1985. Monoclonal antibodies specific for adenovirus early region 1A proteins: extensive heterogeneity in early region 1A products. J Virol 55:533–546. https://doi.org/10.1128/JVI.55.3.533-546.1985
39. Vijayalingam S, Subramanian T, Zhao L-J, Chinnadurai G. 2016. The cellular protein complex associated with a transforming region of E1A contains c-MYC. J Virol 90:1070–1079. https://doi.org/10.1128/JVI.02039-15
40. Grand RJ, Turnell AS, Mason GG, Wang W, Milner AE, Mymryk JS, Rookes SM, Rivett AJ, Gallimore PH. 1999. Adenovirus early region 1A protein binds to mammalian SUG1-a regulatory component of the proteasome. Oncogene 18:449–458. https://doi.org/10.1038/sj.onc.1202304
41. Burleigh K, Maltbaek JH, Cambier S, Green R, Gale M, James RC, Stetson DB. 2020. Human DNA-PK activates a STING-independent DNA sensing pathway. Sci Immunol 5:eaba4219. https://doi.org/10.1126/sciimmunol.aba4219
42. Jin J, Arias EE, Chen J, Harper JW, Walter JC. 2006. A family of diverse Cul4-Ddb1-interacting proteins includes Cdt2, which is required for S phase destruction of the replication factor Cdt1. Mol Cell 23:709–721. https://doi.org/10.1016/j.molcel.2006.08.010
43. Soucy TA, Smith PG, Milhollen MA, Berger AJ, Gavin JM, Adhikari S, Brownell JE, Burke KE, Cardin DP, Critchley S, et al. 2009. An inhibitor of NEDD8-activating enzyme as a new approach to treat cancer. Nature 458:732–736. https://doi.org/10.1038/nature07884
44. Yamamoto SP, Okawa K, Nakano T, Sano K, Ogawa K, Masuda T, Morikawa Y, Koyanagi Y, Suzuki Y. 2011. Huwe1, a novel cellular interactor of Gag-Pol through integrase binding, negatively influences HIV-1 infectivity. Microbes Infect 13:339–349. https://doi.org/10.1016/j.micinf.2010.12.002
45. Kim SG, Hoffman GR, Poulogiannis G, Buel GR, Jang YJ, Lee KW, Kim B-Y, Erikson RL, Cantley LC, Choo AY, Blenis J. 2013. Metabolic stress controls mTORC1 lysosomal localization and dimerization by regulating the TTT-RUVBL1/2 complex. Mol Cell 49:172–185. https://doi.org/10.1016/j.molcel.2012.10.003
46. Tsukamoto AS, Ponticelli A, Berk AJ, Gaynor RB. 1986. Genetic mapping of a major site of phosphorylation in adenovirus type 2 E1A proteins. J Virol 59:14–22. https://doi.org/10.1128/JVI.59.1.14-22.1986
47. Lin R, Heylbroeck C, Pitha PM, Hiscott J. 1998. Virus-dependent phosphorylation of the IRF-3 transcription factor regulates nuclear translocation, transactivation potential, and proteasome-mediated degradation. Mol Cell Biol 18:2986–2996. https://doi.org/10.1128/MCB.18.5.2986
48. Hemmi H, Takeuchi O, Kawai T, Kaisho T, Sato S, Sanjo H, Matsumoto M, Hoshino K, Wagner H, Takeda K, Akira S. 2000. A toll-like receptor recognizes bacterial DNA. Nature 408:740–745. https://doi.org/10.1038/35047123
49. Hu M-M, Shu H-B. 2020. Innate immune response to cytoplasmic DNA: mechanisms and diseases. Annu Rev Immunol 38:79–98. https://doi.org/10.1146/annurev-immunol-070119-115052
50. Chen J, Morral N, Engel DA. 2007. Transcription releases protein VII from adenovirus chromatin. Virology 369:411–422. https://doi.org/10.1016/j.virol.2007.08.012
51. Ostapchuk P, Suomalainen M, Zheng Y, Boucke K, Greber UF, Hearing P. 2017. The adenovirus major core protein VII is dispensable for virion assembly but is essential for lytic infection. PLoS Pathog 13:e1006455. https://doi.org/10.1371/journal.ppat.1006455
52. Zimmermann H, Degenkolbe R, Bernard HU, O'Connor MJ. 1999. The human papillomavirus type 16 E6 oncoprotein can down-regulate p53 activity by targeting the transcriptional coactivator CBP/p300. J Virol 73:6209–6219. https://doi.org/10.1128/JVI.73.8.6209-6219.1999
53. Eckner R, Ludlow JW, Lill NL, Oldread E, Arany Z, Modjtahedi N, DeCaprio JA, Livingston DM, Morgan JA. 1996. Association of p300 and CBP with simian virus 40 large T antigen. Mol Cell Biol 16:3454–3464. https://doi.org/10.1128/MCB.16.7.3454
54. Nemethova M, Wintersberger E. 1999. Polyomavirus large T antigen binds the transcriptional coactivator protein p300. J Virol 73:1734–1739. https://doi.org/10.1128/JVI.73.2.1734-1739.1999
55. Timms RT, Zhang Z, Rhee DY, Harper JW, Koren I, Elledge SJ. 2019. A glycine-specific N-degron pathway mediates the quality control of protein N-myristoylation. Science 365:eaaw4912. https://doi.org/10.1126/science.aaw4912
56. Jean F, Pilgrim D. 2017. Coordinating the uncoordinated: UNC119 trafficking in cilia. Eur J Cell Biol 96:643–652. https://doi.org/10.1016/j.ejcb.2017.09.001
57. Bouhamdan M, Benichou S, Rey F, Navarro JM, Agostini I, Spire B, Camonis J, Slupphaug G, Vigne R, Benarous R, Sire J. 1996. Human immunodeficiency virus type 1 Vpr protein binds to the uracil DNA glycosylase DNA repair enzyme. J Virol 70:697–704. https://doi.org/10.1128/JVI.70.2.697-704.1996
58. Horejsí Z, Takai H, Adelman CA, Collis SJ, Flynn H, Maslen S, Skehel JM, de Lange T, Boulton SJ. 2010. CK2 phospho-dependent binding of R2TP complex to TEL2 is essential for mTOR and SMG1 stability. Mol Cell 39:839–850. https://doi.org/10.1016/j.molcel.2010.08.037
59. Rajendra E, Garaycoechea JI, Patel KJ, Passmore LA. 2014. Abundance of the fanconi anaemia core complex is regulated by the RuvBL1 and RuvBL2 AAA+ ATPases. Nucleic Acids Res 42:13736–13748. https://doi.org/10.1093/nar/gku1230

60. Wood MA, McMahon SB, Cole MD. 2000. An ATPase/helicase complex is an essential cofactor for oncogenic transformation by c-Myc. Mol Cell 5:321–330. https://doi.org/10.1016/s1097-2765(00)80427-x
61. Berk AJ. 2005. Recent lessons in gene expression, cell cycle control, and cell biology from adenovirus. Oncogene 24:7673–7685. https://doi.org/10.1038/sj.onc.1209040
62. Xu T, Park SK, Venable JD, Wohlschlegel JA, Diedrich JK, Cociorva D, Lu B, Liao L, Hewel J, Han X, Wong CCL, Fonslow B, Delahunty C, Gao Y, Shah H, Yates JR. 2015. ProLuCID: an improved SEQUEST-like algorithm with enhanced sensitivity and specificity. J Proteomics 129:16–24. https://doi.org/10.1016/j.jprot.2015.07.001
63. Tabb DL, McDonald WH, Yates JR. 2002. DTASelect and contrast: tools for assembling and comparing protein identifications from shotgun proteomics. J Proteome Res 1:21–26. https://doi.org/10.1021/pr015504q